

## Research Article

# Influence of Microstructural Characteristics on Wear and Corrosion Behaviour of $\text{Si}_3\text{N}_4$ -Reinforced Al2219 Composites

C. J. Manjunatha,<sup>1</sup> C. Durga Prasad ,<sup>2</sup> Harish Hanumanthappa,<sup>2</sup> A. Rajesh Kannan ,<sup>3</sup> Dhanesh G. Mohan ,<sup>4</sup> Bharath Kumar Shanmugam,<sup>5</sup> and C. Venkategowda<sup>1</sup>

<sup>1</sup>Atria Institute of Technology, Bengaluru, Karnataka 560024, India

<sup>2</sup>RV Institute of Technology and Management, Bengaluru, Karnataka 560076, India

<sup>3</sup>Hanyang University, 55, Hanyangdaehak-ro, Ansan 15588, Gyeonggi-do, Republic of Korea

<sup>4</sup>Zhengzhou Research Institute, Harbin Institute of Technology, Zhengzhou-450046, China

<sup>5</sup>RNS Institute of Technology, Bengaluru, Karnataka 560098, India

Correspondence should be addressed to Dhanesh G. Mohan; [dgmohan@hit.edu.cn](mailto:dgmohan@hit.edu.cn)

Received 6 January 2023; Revised 6 February 2023; Accepted 9 February 2023; Published 20 February 2023

Academic Editor: Tushar Sonar

Copyright © 2023 C. J. Manjunatha et al. This is an open access article distributed under the Creative Commons Attribution License, which permits unrestricted use, distribution, and reproduction in any medium, provided the original work is properly cited.

The fabrication of the Al2219 +  $\text{Si}_3\text{N}_4$  composites was done by means of stir casting process. The specimen was subjected to microstructural studies. The density of  $\text{Si}_3\text{N}_4$  employed in the fabrication of the composites has been evaluated. Generally, the density of the composites increases as the weight percent of  $\text{Si}_3\text{N}_4$  increases. TGA and DTA were performed at temperatures ranging from 30°C to 800°C, with some mass loss noted as well as the thermal stability of an AA2219 matrix improved. Under various parameters of applied load, operating duration, and speed, the wear behaviour of the produced aluminium matrix composite (AMC) was examined. Corrosion behaviour was examined using potentiodynamic polarization curve data, and it was discovered that the rate of corrosion decreases with increasing  $\text{Si}_3\text{N}_4$  content, adding to the AA2219 matrix. The research work is intended to produce a totally new composite material with various compositions of reinforcement and to investigate their mechanical properties and a result of simulation.

## 1. Introduction

A composite material is composed of two or more main components with chemical or physical qualities that are quite distinct from one another and that, when combined, produce a material with characteristics that are specific to each of the constituent parts [1, 2]. Several factors, including the new material's superior strength, lighter weight, and more affordable price compared to the old materials, may influence the decision [3]. Aside from worktops, cultured marble, granite, and bathtubs, there are also shower stalls, tanks for storage, and bathtubs. There are many examples of the application of composites, which can apply in different environments [4]. Composite materials are used to construct structures such as buildings, bridges, boat hulls, and ships [5–7].

The main advantage of a composite material over a monolithic metal is the special synthesis of a number of properties that are unusual in traditional materials, improved fatigue resistance, higher stiffness-to-weight ratio, and higher strength-to-weight ratio [1, 2, 8–10]. Improved thermal expansion and corrosion resistance, better optical and magnetic properties, wear resistance, and fracture toughness are only a few of the special combination qualities. Their wide range of commands requires an unusual combination of traits in order to give appropriate properties for the composite [11–13]. In addition, the usage of lightweight materials is becoming more popular since they are easier to produce, take up less room, need fewer components during assembly, look better, and offer superior protection against corrosion assault. These reasons have inspired the present generation of developers to produce novel composites,

which are currently produced in vast quantities and to exacting standards [14–18]. The bulk of the structural loads are carried by fibrous reinforcement, which provides macroscopic stiffness and strength. As of now, composite materials assume a significant part in aviation, cars, and other design applications because of their great solidarity-to-weight and modulus-to-weight proportions [19–22].

The requirement for quality casting also increases to a high standard without any defects like blow holes or porosity in the annealing condition. Experts with extensive expertise recommend utilizing a cognitive approach to melting and modeling [23–26]. The cognitive method provides a one-of-a-kind chance to incorporate all found components and deal with them collaboratively and concurrently [27, 28]. In light of the foregoing discussion, the current work's objective is to investigate the microstructural characteristics of an aluminium alloy called AA2219 that has been reinforced with varying concentrations of  $\text{Si}_3\text{N}_4$  (0, 3, 6, and 9) particles using the high energy stir casting method. Further the produced samples were tested for wear and corrosion characteristics. The benefit of using  $\text{Si}_3\text{N}_4$  as a reinforcement material to interface bonding strength is the main reason for the composite relatively high specific mechanical properties.

## 2. Materials and Methods

**2.1. Materials and Casting Process.** By weighing the components of the composite, which is made of silicon nitride as reinforcement and aluminium alloy 2219 as the base material, we were able to determine their respective proportions of (0%, 3%, 6%, and 9%).  $\text{Si}_3\text{N}_4$  is a ceramic material with a low density ( $3.1 \text{ g/cm}^3$ ) that has excellent mechanical strength and hardness, good thermal and chemical stability, and strong wear and corrosion resistance. Beginning with stirring to reach the melting point of black lead in a coal-fired chamber, the composite is prepared. The molten metal matrix is continuously stirred to produce a solid composite. This is frequently put directly into the mould to cause coagulation. The fuel employed for the fabrication to soften was coal.

**2.2. Microstructural Investigation.** The specimens for scanning electron microscope (SEM) were polished in accordance with industry standards. Specimens were polished with 1/0, 2/0, and 3/0 diamond paste after being ground with 80–4000 grade emery paper. Keller's reagent was then used to etch the specimen. Metals have a preferred microstructure obtained by a specified processing or heat treatment to achieve desired material properties (ASTM E3 and E112).

**2.3. Thermal Analysis.** Thermal analysis studies how the characteristics of materials vary with temperature. Physical variations include melting, evaporation, and crystallization, as well as transitions between crystalline structures, variations in metal composition microstructure, and mechanical behaviour modification. The equipment used for the TGA is EXSTAR 6300 instrument.

**2.4. Wear Test.** The wear samples were evaluated in a dry environment. Maintaining a constant sliding distance, the sliding pressure is changed by increasing the weights. The equipment comprises a spinning disc (made of EN24 steel with a hardness of BHN 229 and a diameter of 200 mm) that serves as the counter surface over which the test specimens or pins move. The wear test was carried out at sliding distances 600, 1800, 2400, and 3000 mm, respectively. The specimen was held in place, and then the load was applied to the specimen. The dimensions of the sample for the wear test are diameter 10 mm and length 50.

**2.5. Corrosion Test.** For corrosion tests, matrix material composites and aluminium alloy  $\text{Si}_3\text{N}_4$  were immersed for 28 days in a 3.5 percent electrolyte solution. The mass loss of the materials was used to calculate corrosion rates (mm/year). After the examination, the samples were washed with 50 vol percent nitric acid ( $\text{HNO}_3$ ), dried, and weighed. The specimens were cut into circular discs with a 3 mm thickness and a 10 mm diameter during the potentiodynamic examination. A small opening is used to place specimens in a corrosion cell for electrical connection. Corrosion experiments were carried out in a 3.5 percent NaCl solution using a CHI 604D electrochemical workstation (CH Instruments, Inc.) with a Ag/AgCl reference electrode and platinum wire as a counter electrode.

## 3. Results and Discussion

**3.1. Microstructure Analysis.** Visual inspection through an inverted metallurgical microscope is done for pure aluminium and different compositions of  $\text{Si}_3\text{N}_4$ . A microstructure is a small-scale material structure viewed through a microscope at magnifications greater than 25. The impact of a microstructure on the physical and mechanical characteristics of a material is largely determined by the lack of flaws present in the structure. Figures 1(a)–1(d) represent a SEM picture of as-cast and Al2219 +  $\text{Si}_3\text{N}_4$  composites magnification of 200 $\times$  it shows the uniform distributions and also a dendritic structure is observed in SEM micrographs. Particles have almost spherical shapes, whereas a black spot indicates particle clustering and porosity at certain points.

**3.2. Thermal Analysis.** Thermal analysis was used to find out thermal stability of the material. The experiments were carried out using simultaneous TGA/DTA test by a temperature range of 30°C to 800°C.

From Figure 2, the TGA/DTA graph, TGA curve shows that there was 7.3% loss of mass in the unreinforced AA2219, and DTA curve shows the two peaks recorded at 64.0°C and 126.2°C, thus two exothermic reactions occurs in unreinforced AA2219.

Figure 3 shows the 3wt.%  $\text{Si}_3\text{N}_4$  TGA/DTA graph, the TGA curve represents the decrease of the level of decomposition rate. However, when the reinforcement is added, it can be decomposed, which indicates 2.5% mass

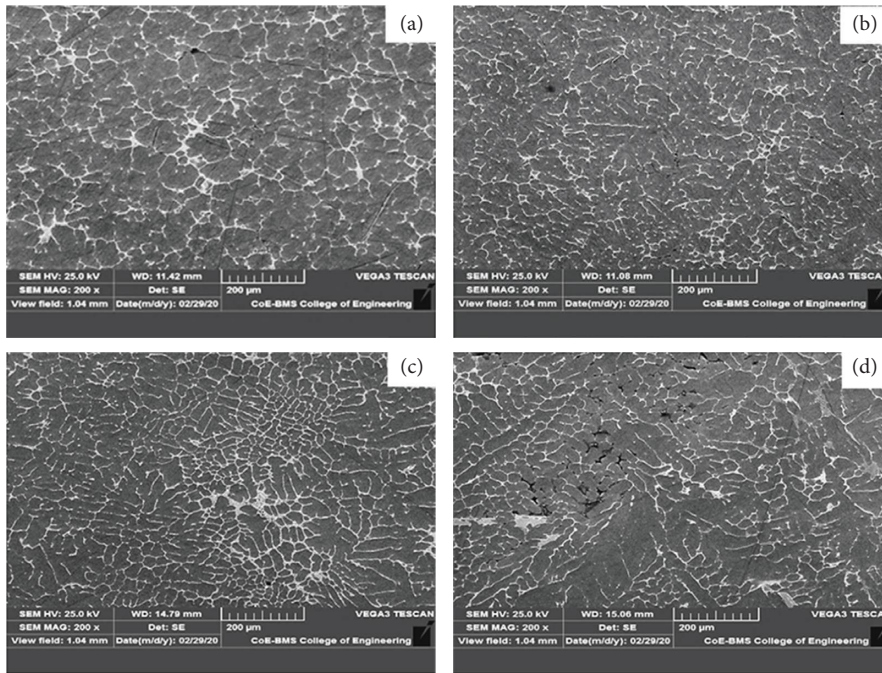


FIGURE 1: SEM images at 200x: (a) as-cast Al2219 alloy, (b) Al2219 + 3wt.% Si<sub>3</sub>N<sub>4</sub>, (c) Al2219 + 6wt.% Si<sub>3</sub>N<sub>4</sub>, and (d) Al2219 + 9wt.% Si<sub>3</sub>N<sub>4</sub>.

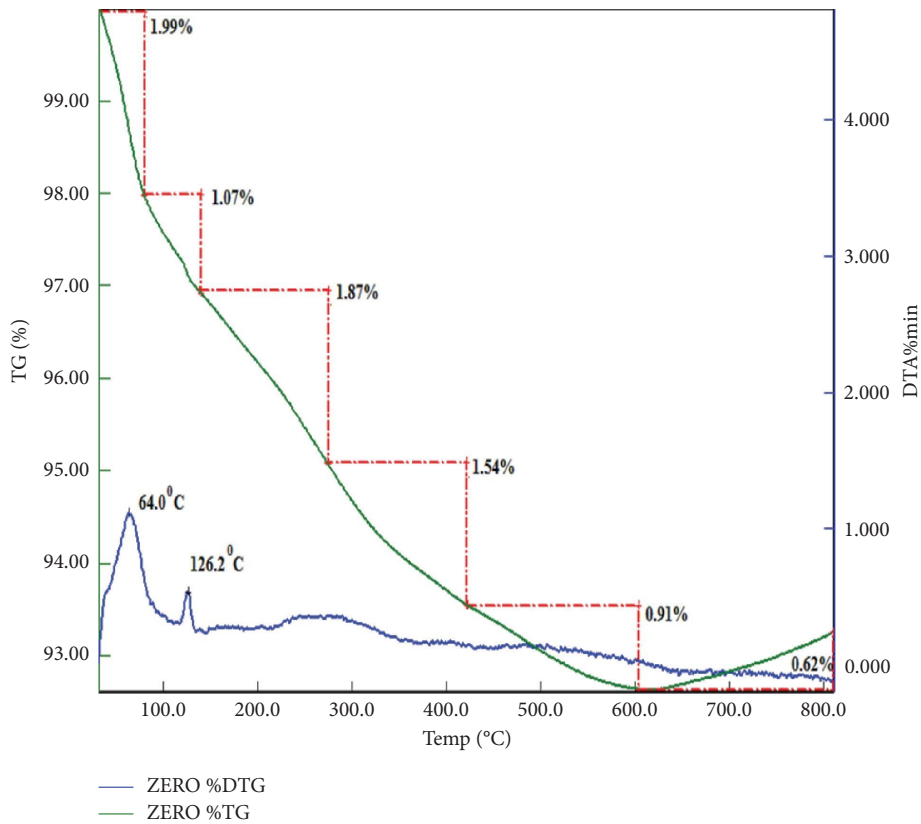


FIGURE 2: 0% TGA and DTA analysis.

loss reduction and the DTA curve shows one peak, such as exothermic reaction occurring at 43.1°C at 3wt.% Si<sub>3</sub>N<sub>4</sub>.

Figure 4 shows the 6wt.% Si<sub>3</sub>N<sub>4</sub> TGA/DTA graph, the TGA curve shows the material was about 4.4% weight loss reduction, and the DTA analysis indicates one peak observed

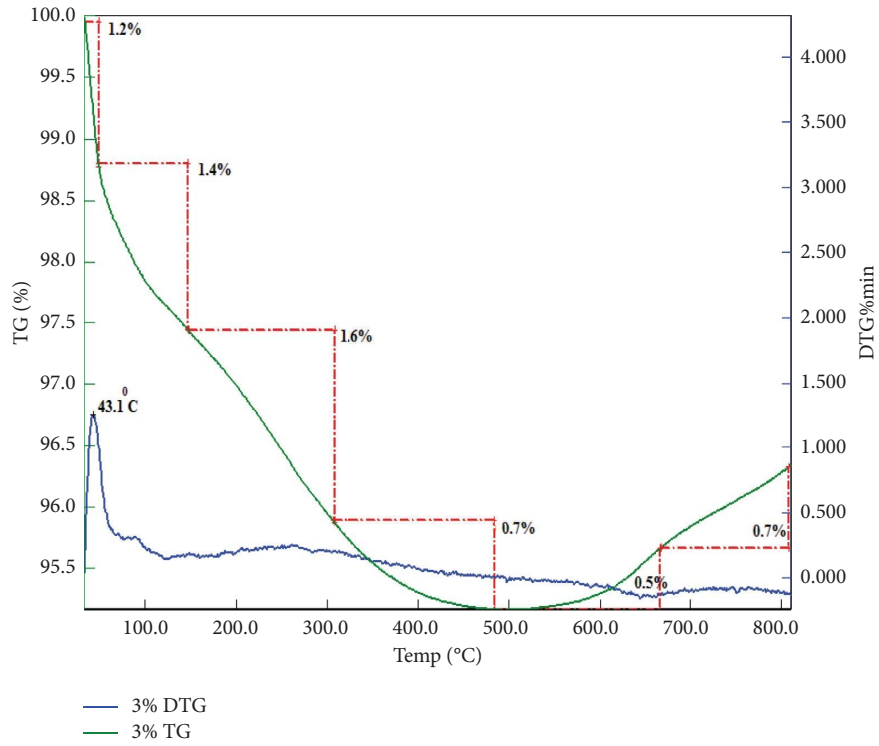


FIGURE 3: 3wt.% TGA and DTA analysis.

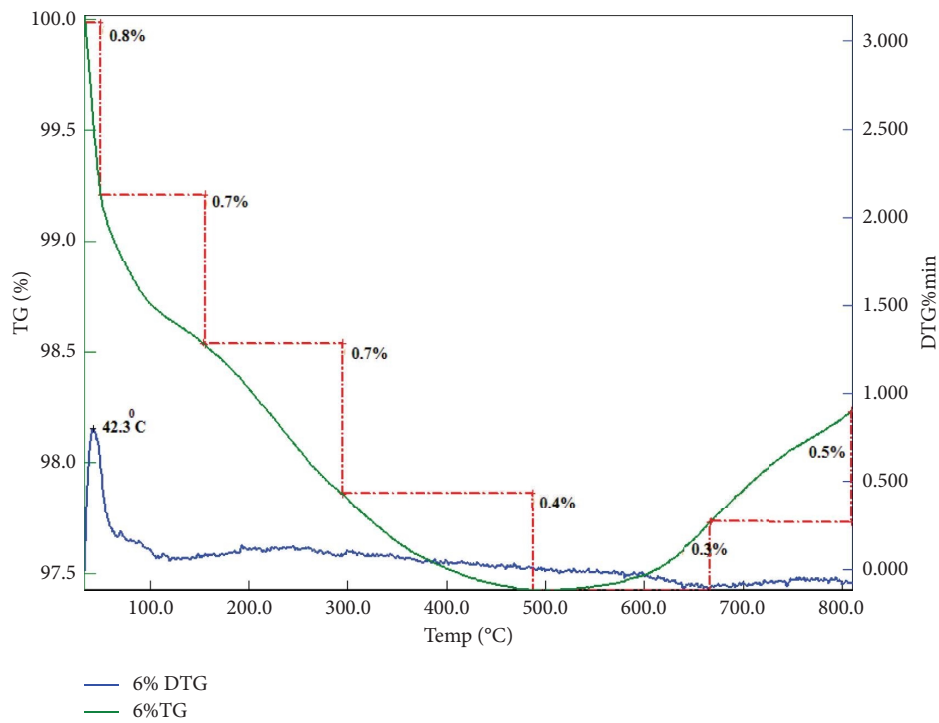


FIGURE 4: 6wt.% TGA and DTA analysis.

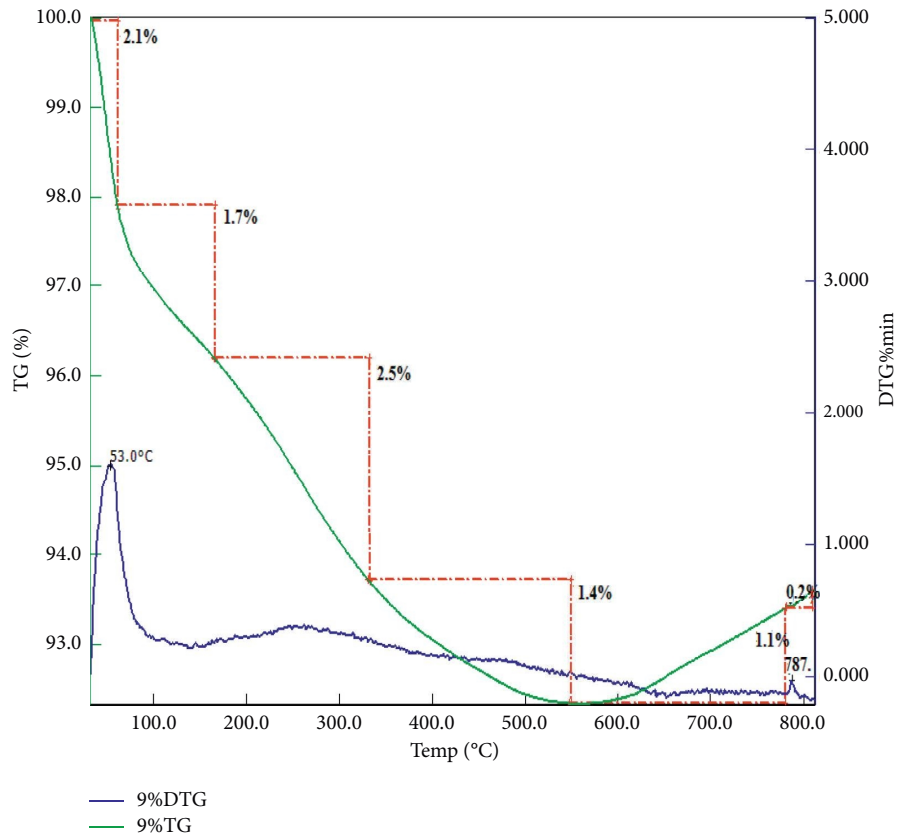


FIGURE 5: 9wt.% TGA and DTA analysis.

such as exothermic reaction occurring at 42.3°C at 6wt.%  $\text{Si}_3\text{N}_4$ .

Figure 5 shows the 9wt.%  $\text{Si}_3\text{N}_4$  of TGA/DTA graph, the TGA curve shows the 7.6% mass loss and the DTA analysis shows the two peaks recorded at 53.0°C and 787.0°C, respectively. The thermal stability thus obtained is higher than that of AA2219. This demonstrates how the use of  $\text{Si}_3\text{N}_4$  benefited in material savings for high temperature uses by decreasing the mass loss with an appropriate  $\text{Si}_3\text{N}_4$  quantity of 3%.

TGA and DTA are shown in Figures 2–5. From the analysis, it was observed that the temperature rate decreased, which in turn initiated some amount of mass loss around 130°C, and it ended at around 849.620°C. A differential thermal analyzer (DTA) and a thermogravimetric analyzer were used to investigate the thermal response of unreinforced AA2219 and produced AA2219– $\text{Si}_3\text{N}_4$  composites (TGA).

**3.3. Wear Analysis.** The outcome of the wear studies, in which the reinforcement, applied stress, sliding velocity, and sliding distance were varied conditions to evaluate the wear rate of the AA2219 +  $\text{Si}_3\text{N}_4$ . The results of the tests and wear analysis show that the wear behaviour of the AA2219 +  $\text{Si}_3\text{N}_4$  composites at 20 N and 40 N, respectively, is affected by the weight percentage of  $\text{Si}_3\text{N}_4$  and the sliding speed.

Figures 6 and 7, which are typical graphs calculated based on wear rate data, indicate the impact of the silicon nitride ( $\text{Si}_3\text{N}_4$ ) content on the wear properties of AA2219 +  $\text{Si}_3\text{N}_4$  particulate for a wear test at rotational speeds of 300, 600, and 900 rpm with weights of 20 and 40 N. The percentage of  $\text{Si}_3\text{N}_4$  (0%, 3%, 6%, and 9%) dispersion determines the wear rate of the AA2219 +  $\text{Si}_3\text{N}_4$  composites. For loadings of 20 N and 40 N, it was discovered that the wear rate decreased when  $\text{Si}_3\text{N}_4$  content rose from 3 to 6 wt%. However, for both the 20 N and 40 N load, there is an increase in the wear rate for the 9 wt% of  $\text{Si}_3\text{N}_4$  compared to the 6 wt% reinforcement. For the composite containing 6 wt%  $\text{Si}_3\text{N}_4$  dispersoid in the as-cast as seen, the weighted rate by wear is minimal. As illustrated in Figures 6 and 7, the wear rate remained nearly constant at lower weights with an increase in rpm. Comparatively, AA2219 without dispersoid demonstrated a low wear rate, however this loss gradually diminished. As seen in the aforementioned images, Figures 6 and 7, the wear resistance may stabilize reasonably quickly due to hard  $\text{Si}_3\text{N}_4$  particles scattered in the base matrix.

**3.4. Worn Out Surface Analysis.** Figures 8(a)–8(d) depict worn out surface analysis for the surface of as-cast AA2219 alloy and AA2219-3, 6, and 9wt. %  $\text{Si}_3\text{N}_4$  composites examined using a SEM after a load of 20 N and 40 N at 300, 600, and 900 rpm. Figure 8(a) illustrates that some of the

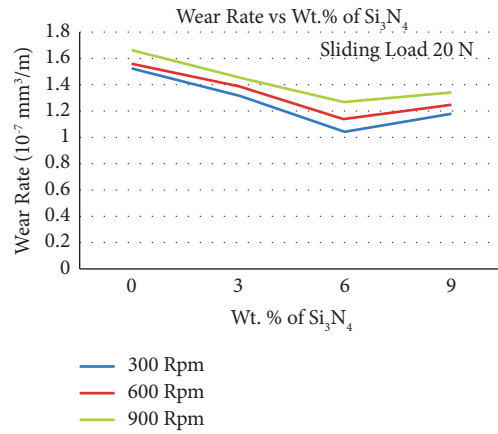


FIGURE 6: The wear behaviour of AA2219/Si<sub>3</sub>N<sub>4</sub> composites at 20 N at different speeds.

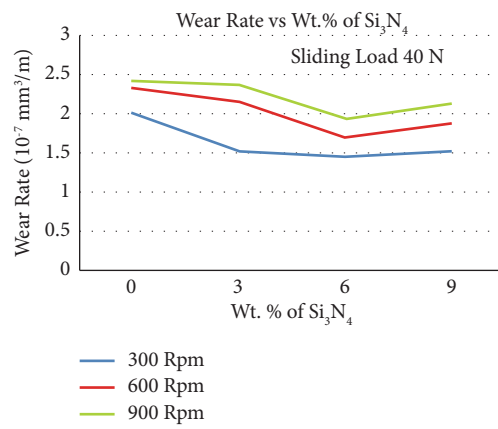


FIGURE 7: The wear behaviour of AA2219/Si<sub>3</sub>N<sub>4</sub> composites at 40 N at different speeds.

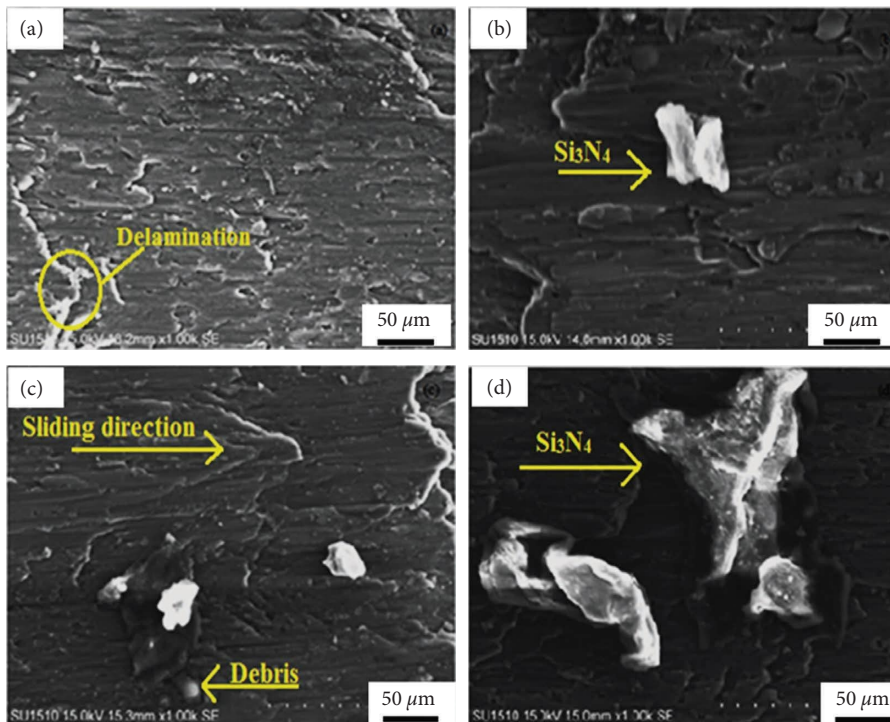


FIGURE 8: (a) As-cast Al2219 alloy, (b) Al2219 + 3wt.% Si<sub>3</sub>N<sub>4</sub>, (c) Al2219 + 6wt.% Si<sub>3</sub>N<sub>4</sub>, and (d) Al2219 + 9wt.% Si<sub>3</sub>N<sub>4</sub>.



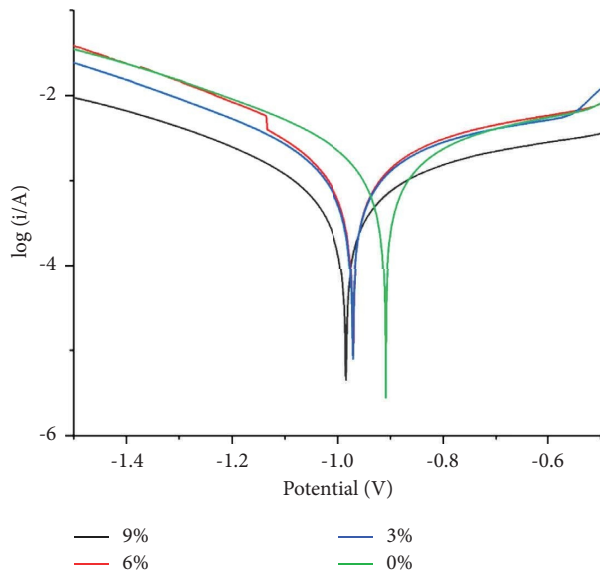


FIGURE 9: Polarization curves for Al-Si<sub>3</sub>N<sub>4</sub> alloy matrix and composites with varying weight percentages of Al<sub>2</sub>O<sub>3</sub> particles evaluated in 3.5% NaCl.

areas in the as-cast AA2219 alloy are damaged. When a greater load is applied, the number of grooves formed at the worn surface of the matrix alloy grows dramatically, resulting in delamination and plastic deformation wear in the specimens. Figures 8(b)–8(d) shows the amount of grooving on the surfaces of the AA2219 alloy composites. The grooves are narrow as the Si<sub>3</sub>N<sub>4</sub> concentration increases, indicating decreased material loss when compared to the AA2219 base matrix material.

**3.5. Corrosion Analysis.** When metal come in contact with the corrosion atmosphere, it makes the electrical reaction into chemical reaction because destruction of materials takes place. The corrosion test is conducted to find out behaviour of materials in an environment which includes NaCl solution.

The potentiodynamic polarization curve for AA2219 with and without Si<sub>3</sub>N<sub>4</sub> reinforcement is shown in Figure 9.

Figure 10 shows the corrosion rate versus weight percentage of the composite. The corrosion rate was reduced with the addition of Si<sub>3</sub>N<sub>4</sub>, demonstrating the material's favorable impact in preventing corrosion. The ceramic Si<sub>3</sub>N<sub>4</sub> inert characteristics make it corrosion resistant. The addition of reinforcement reduced the corrosion rate, indicating that it has a beneficial effect on the material in terms of preventing corrosion. The addition of reinforcement reduced the corrosion rate, indicating that it has a beneficial effect on the material in terms of preventing corrosion. The weight loss corrosion rate of the matrix and composites in different concentrations. The corrosion rate decreases with an increase in exposure time irrespective of the matrix and percentage of reinforcement. The rate of corrosion decreases as there is an increase in the reinforcement content. The corrosion product formed on the surface of the composites was removed. Due to the nonporous oxide layer of the

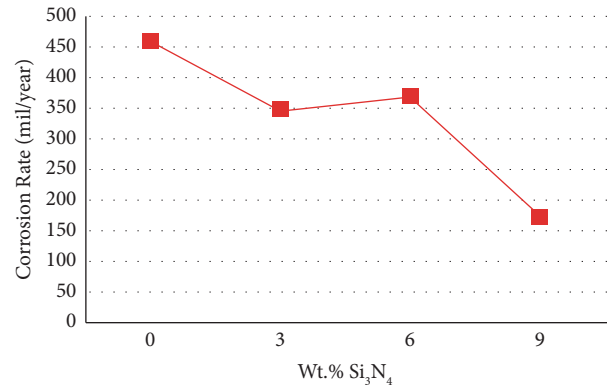


FIGURE 10: Corrosion rate vs wt.% Si<sub>3</sub>N<sub>4</sub>.

aluminium, the rate of corrosion decreases gradually. Si<sub>3</sub>N<sub>4</sub> particles are inert and will not affect the coercion mechanism of the metal matrix composite. The results indicate that as the percentage of Si<sub>3</sub>N<sub>4</sub> increases, corrosion rate decreases. This shows that the corrosion rate directly or indirectly affects the corrosion property of the composites. The base matrix and the reinforcement interphase is the weakest part of the particulate reinforced composite. Hence, in the corrosion process, the nature of the bond whether weak or strong is critical.

#### 4. Conclusions

- (i) The SEM analysis of AA2219 + Si<sub>3</sub>N<sub>4</sub> composite indicated that there was a good bonding in the composites and uniform distribution of Si<sub>3</sub>N<sub>4</sub> particles in AA2219. Furthermore, it was observed that the agglomeration of silicon nitride is greater in 9 wt% of Si<sub>3</sub>N<sub>4</sub> MMC than in 3wt% of Si<sub>3</sub>N<sub>4</sub>.
- (ii) Load factor and sliding speed have the most influence on the wear rate of the produced composite. It was observed that by increasing the load and sliding speed, there was a considerable decrease in the wear rate. When compared to as-cast AA2219 base metal, the produced composite containing 3 and 6 wt.% of Si<sub>3</sub>N<sub>4</sub> has a low rate of wear and observed the rise in the wear rate at 9wt. % of Si<sub>3</sub>N<sub>4</sub>
- (iii) As the load increases, the number of grooves formed on the worn surface of the composite increases, and delamination occurs, resulting in plastic deformation wear in the specimen. Furthermore, it was observed that the reduction in grooves on the surface of the specimen with an increase in wt.% Si<sub>3</sub>N<sub>4</sub> reinforcement led to low removal of the material on the surface as compared to the as-cast AA2219 base metal matrix.
- (iv) The thermal response of as-cast AA2219 and the produced composite (AA2219 + Si<sub>3</sub>N<sub>4</sub>) indicates that the developed composite improves the thermal stability of the aluminium alloy matrix, which helps in the use of high-temperature applications.
- (v) The developed composite material was subjected to a corrosion test. The addition of Si<sub>3</sub>N<sub>4</sub> (3, 6, and 9

wt. % Si<sub>3</sub>N<sub>4</sub>) reduced the corrosion rate, indicating that it has a beneficial effect on the material in terms of preventing corrosion.

## Data Availability

The data supporting the findings of this study are available within the article.

## Ethical Approval

This article is the original work of all authors, which has never been published, has only been submitted to this journal, and if approved, will not be submitted to any other journal in any language. It was created with the help of all authors.

## Consent

Informed consent was received from all participants.

## Conflicts of Interest

The authors declare that they have no conflicts of interest.

## Authors' Contributions

All authors contributed to the study conception and design. Material preparation, data collection, and data analysis were performed by C. J. Manjunatha, Durga Prasad C, Harish Hanumanthappa, and Bharath Kumar Shanmugam. The first draft of the manuscript was written by C. J. Manjunatha, Durga Prasad C, and Harish Hanumanthappa. The draft of the manuscript was reviewed by Venkategowda C, Rajesh Kannan A, and Dhanesh G. Mohan. All authors read and approved the final manuscript.

## References

- [1] C. J. Manjunatha and B. Venkata Narayana, "Experimental analysis of mechanical properties of aluminium alloy 2219 reinforced with Si<sub>3</sub>N<sub>4</sub>," *International Journal of Innovative Technology and Exploring Engineering ijitee*, vol. 9, no. 2, 2019.
- [2] G. Ramanan, J. Edwin Raja Dhas, M. Ramachandran, and G. Diju Samuel, "Influence of activated carbon particles on microstructure and thermal analysis of aa7075 metal matrix composites," *Rasayan Journal Chem*, vol. 10, no. 2, pp. 375–384, 2017.
- [3] A. C. Gowda, P. G. Koppad, D. Sethuram, and R. Keshavamurthy, "Morphology studies on mechanically milled aluminium reinforced with B<sub>4</sub>C and CNTs," *Silicon*, vol. 11, no. 2, pp. 1089–1098, 2019.
- [4] C. J. Manjunatha, V. Narayana, and D. B. P. Raja, "Investigating the effect of Si<sub>3</sub>N<sub>4</sub> reinforcement on the morphological and mechanical behavior of AA2219 alloy," *Silicon*, vol. 14, no. 6, pp. 2655–2667, 2021.
- [5] J. Harti, T. B. Prasad, M. Nagaral, and K. Niranjan Rao, "Hardness and tensile behavior of Al2219-TiC metal matrix composites," *Journal of Mechanical Engineering and Automation*, vol. 6, no. 5, pp. 8–12, 2016.
- [6] C. J. Manjunatha, B. Venkata Narayana, D. Bino Prince Raja, and R. S. Rimal Isaac, "Tribological, thermal and corrosive behaviour of aluminium alloy 2219 reinforced by Si<sub>3</sub>N<sub>4</sub> nanosized powder," *Silicon*, vol. 14, no. 8, pp. 4325–4336, 2021.
- [7] V. Ramakoteswara Rao, N. Ramanaiah, and M. S. Mohammed Moulana, "Mechanical and tribological properties of AA7075-TiC metal matrix composites under heat treated (T6) and cast conditions," *JMRTEC*, vol. 227, p. 7, 2016.
- [8] S. Suresh, N. Shenbaga Vinayaga Moorthi, N. Selvakumar, and S. C. Vettivel, "Tribological, tensile and hardness behavior of Tib2 reinforced aluminium metal matrix composite," *Journal of the Balkan Tribological Association*, vol. 20, no. 3, pp. 380–394, 2014.
- [9] S. Zhu, T. Luo, T. Zhang, Y. Li, and Y. Yang, "Effects of Cu addition on the microstructure and mechanical properties of as-cast and heat treated Mg-6Zn-4Al magnesium alloy," *Materials Science and Engineering A*, vol. 689, pp. 203–211, 2017.
- [10] V. K. Singh, S. Chauhan, P. C. Gope, and A. K. Chaudhary, "Enhancement of wettability of aluminum based silicon carbide reinforced particulate metal matrix composite," *High Temperature Materials and Processes*, vol. 10, pp. 163–170, 2014.
- [11] S. Suresha and B. K. Sridhara, "Wear characteristics of hybrid aluminium matrix composites reinforced with graphite and silicon carbide particulates," *Composites Science and Technology*, vol. 70, no. 11, pp. 1652–1659, 2010.
- [12] V. C. Uvaraja and N. Natarajan, "Optimization of friction and wear behaviour in hybrid metal matrix composites using taguchi technique," *Journal of Minerals and Materials Characterization and Engineering*, vol. 11, no. 8, pp. 757–768, 2012.
- [13] T. Dileep and P. N. S. Srinivas, "Enhancement of mechanical, microscopic and tribological properties of hybrid metal matrix composite reinforced with alumina, graphite and silicon carbide," *Internation Journal Latest Eng Res App*, vol. 1, pp. 41–49, 2016.
- [14] V. R. Rao, N. Ramanaiah, and M. Sarcar, "Moulana M and Mechanical and tribological properties of AA7075-TiC metal matrix composites under heat treated (T6) and cast conditions," *Journal of Materials Research and Technology*, vol. 5, pp. 1–7, 2016.
- [15] C. Venkategowda, H. Hanumanthappa, C. D. Prasad, B. K. Shanmugam, T. N. Sreenivasa, and M. S. R. Kumar, "High-temperature tribological studies on hot forged Al6061-Tib2 in-situ composites," *Journal of Bio and Tribo-Corrosion*, vol. 8, no. 4, p. 101, 2022.
- [16] S. Suresh, S. Vinayaga Moorthi, N. Selvakumar, and S. C. Vettivel, "Tribological tensile and hardness behaviour of Tib2 reinforced aluminium metal matrix composites," *Journal Balk Tribo Assoc*, vol. 20, pp. 380–394, 2014.
- [17] A. Baradeswaran, A. Elayaperumal, and J. Paulo Davim, "Effect of B<sub>4</sub>C on mechanical properties and tribological behaviour of Al6061-B<sub>4</sub>c composites," *Journal Balk Tribol Assoc*, vol. 19, 2013.
- [18] Y. Yusuf Kayali, "Wear and corrosion behaviour of borided and nitride M2 high speed steel," *Journal Balk Tribol Assoc*, vol. 19, pp. 340–353, 2013.
- [19] I. Sulima, I. Jaworska, P. Wyzga, and M. Perek-Nowak, "The influence of reinforcing particles on mechanical and tribological properties and microstructure of the steel-Tib2 composites," *Journal Achiev Mater Manuf Eng*, vol. 48, pp. 52–57, 2010.
- [20] P. Li, Y. Li, Y. Wu, G. Ma, and X. Liu, "Distribution of Tib2 particles and its effect on the mechanical properties of A390



- alloy,” *Materials Science and Engineering A*, vol. 546, pp. 146–152, 2012.
- [21] A. Sreenivasan, S. Paul Vizhian, N. D. Shivakumar, M. Muniraju, and M. Raguraman, “A study of micro structure and wear behaviour of Tib2/Al metal matrix composites,” *Latin American Journal of Solids and Structures*, vol. 8, pp. 1–8, 2011.
- [22] A. Wlodarczyk-Fligier, L. A. Dobrzanski, and M. Adamiak, “Influence of heat treatment on corrosion resistance of PM composite materials,” *Journal Achiev Mater Manuf Eng*, vol. 24, p. 127, 2007.
- [23] S. Suresh, N. Shenbaga Vinayaga Moorthi, S. C. Vettivel, N. Selvakumar, and G. R. jinu, “Effect of graphite addition on mechanical behavior of Al6061/TiB2 hybrid composite using acoustic emission,” *Materials Science and Engineering A*, vol. 612, p. 15, 2014.
- [24] V. Erturun, S. cetin, and O. Sahin, “Investigation of micro structure of aluminium based composite material obtained by mechanical alloying,” *Metals and Materials International*, vol. 1, p. 9, 2020.
- [25] P. C. R. Nunes and L. V. Ramanathan, “Corrosion behavior of alumina-aluminum and silicon carbide-aluminum metal-matrix composites,” *Corrosion*, vol. 51, no. 8, pp. 610–617, 1995.
- [26] F. Toptan, A. C. Alves, I. Kerti, E. Ariza, and L. A. Rocha, “Corrosion and tribocorrosion behaviour of Al–Si–Cu–Mg alloy and its composites reinforced with B4C particles in 0.05M NaCl solution,” *Wear*, vol. 306, no. 2, pp. 27–35, 2013.
- [27] D. G. Kolman and D. P. Butt, “ChemInform abstract: corrosion behavior of a novel SiC/Al2O3/Al composite exposed to chloride environments,” *ChemInform*, vol. 29, no. 10, 2010.
- [28] M. F. Gozzi, E. Radovanovic, I. V. P. Yoshida, and P. Yoshida, “Si3N4/SiC nano composite powder from a pre ceramic polymeric network based on poly (methylsilane) as the sic precursor,” *Materials Research*, vol. 4, no. 1, pp. 13–17, 2001.